In memory of G.N. Petrova

Magnetostratigraphic Data on the Upper Cretaceous of Tuarkyr (Turkmenistan) and Their Implications for the General Paleomagnetic Time Scale

A. Yu. Guzhikov,[1] E. A. Molostovskii,[2] Kh. Nazarov,[3][†] V. A. Fomin,[2] E. Yu. Baraboshkin,[4] and L. F. Kopaevich[4]

[1]*Geological Faculty, Saratov State University, ul. Astrakhanskaya 83, Saratov, 410026 Russia*
[2] *Research Institute of Geology (RIG), Saratov State University (SSU), Saratov, Russia*
[3]*Institute of Geology, Academy of Sciences of Turkmenistan, ul. Gogolya 16, Ashkhabad, 744600 Turkmenistan*
[4] *Geological Faculty, Moscow State University, Vorob'evy gory, Moscow, 119899 Russia*
Received December 20, 2001

Abstract—The Cenomanian–Campanian deposits of Tuarkyr (northwestern Turkmenistan) are studied magnetostratigraphically with a reliable paleontological control. Turonian–Campanian rocks possess a high paleomagnetic stability. The existence of a reversed polarity subzone in the middle Cenomanian and several reversals in the Turonian–Coniacian is confirmed. The Santonian–Campanian of the section is dominated by a reversed polarity. The results of the study point to an intricate magnetic zonation of the Cenomanian–Campanian and, together with the analysis of data on the Upper Cretaceous of other regions, suggest the necessity of revising the Cenomanian–Campanian interval of the magnetostratigraphic time scale, which has been traditionally considered as an interval of a predominantly normal polarity. New data on the Cenomanian–Campanian geomagnetic field regime also suggest that geodynamic models relating the epoch of the quiet Cretaceous field to various geological events should possibly be reexamined.

INTRODUCTION

The Upper Cretaceous interval of the paleomagnetic time scale, except for the Maestrichtian, has been traditionally regarded as an interval of a predominantly normal (N, or n) polarity. In the magnetochronological time scales, the upper part of the $C34$ chron, characterized solely by the N polarity, corresponds to the Cenomanian–Santonian. The $C33$ chron, comprising an anomaly of the reversed (R, or r) polarity, corresponds to the Campanian stage; in the recent variants of reversal time scales [Gradstein and Ogg, 1996; Shreider, 1998], the $C32$ and partially the $C31$ chrons are assigned to the Campanian, which caused the upper part of the stage to appear as an alternating (N/R) polarity interval. The Dzhalal Nr hyperzone[1] in the magnetostratigraphic time scale of the Phanerozoic of the USSR [Molostovskii and Khramov, 1984] is equivalent to the Aptian–Campanian; the hyperzone is complicated in its Upper Cretaceous part by two magnetic R zones: Kul'dzhinskaya at the Santonian–Campanian boundary (analogue of anomaly 33r) and Klyuevskaya in the Coniacian.

New data from the North Caucasus and western Kopet Dagh [Fomin and Eremin, 1993, 1999; Eremin *et al.*, 1995; Fomin, 2000; Fomin and Molostovskii, 2001], southern England [Montgomery *et al.*, 1998], and Germany [Hambach and Krumsiek, 1989] indicate that, compared to the generally accepted ideas, the regime of the geomagnetic field was more complicated in the Cenomanian–Campanian time. Previously unknown R subzones of the middle Cenomanian and lower Turonian have been revealed, the existence of the Coniacian Klyuevskaya R subzone has been confirmed, and the stratigraphic volume of the Kul'dzhinskaya R orthozone (analogue of the 33r anomaly) has been extended to the major part of the Santonian and to the entire lower Campanian. In addition, the presence of numerous microzones of opposite polarities has been established within both N and R zones.

Unlike earlier works by Pergament *et al.* [1971], Vandenberg and Wonders [1980], Krumsiek [1982], and others, who also note repeated reversals in the Cenomanian–Campanian, new polarity determinations have been reliably correlated with zonal units of the General stratigraphic time scale on the basis of macro- and microfauna determinations collected along with paleomagnetic samples. This made it possible to estimate the duration of the $C33r$ chron (the Kul'dzhinskaya zone) at 8 Myr and the duration of the Cenomanian, Turonian, and Coniacian R subzones at 0.4–0.5 to 1 Myr each.

[†]Deceased.
[1]The stratigraphic volume of a hyperzone is comparable with a division, that of an orthozone with a substage or stage, and that of a subzone with a zone of the General stratigraphic time scale [*Stratigraficheskii kodeks*, 1992].
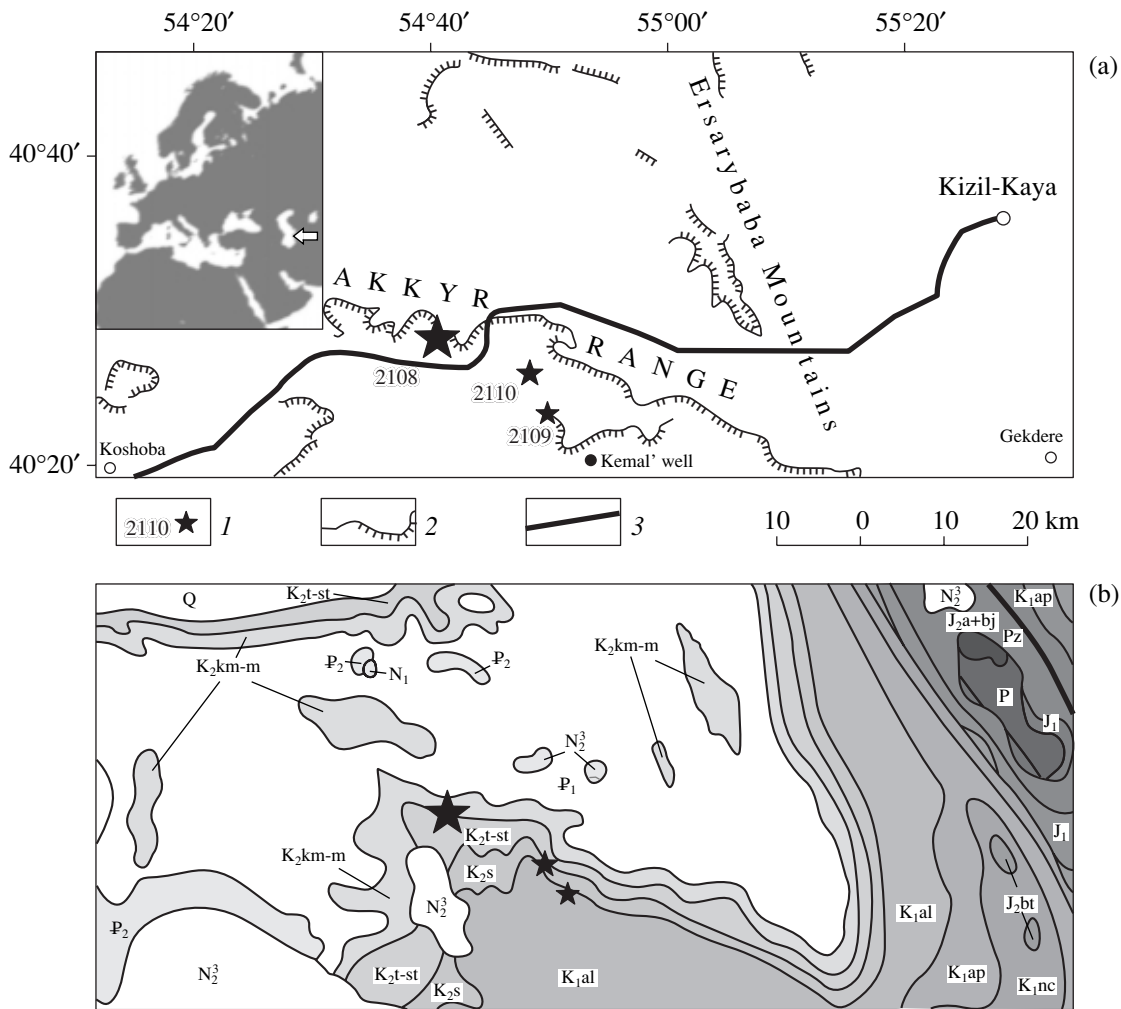
Fig. 1. Topographic (a) and geological (b) schemes of the study region: (*1*) natural exposures studied and observation point numbers; (*2*) escarpments; (*3*) highway.

Disagreement between the new data and the traditional concepts of the Upper Cretaceous scale zonation is of basic importance for elucidating the actual regime of the Late Cretaceous geomagnetic field. Reliable additional information from other regions is necessary for solving this problem. Such a region could well be the Turan plate, where, as distinct from orogens of the Caucasus and Kopet Dagh, Cretaceous deposits have remained virtually undeformed by the Alpine folding (which increases the probability of regional remagnetization of rocks) and are represented by typical platform, rather than geosynclinal, formations. A reference section belonging to the Upper Cretaceous of Tuarkyr was chosen as an object of study. It is characterized by a sufficient stratigraphic completeness and, as is evident from the results of reconnaissance studies reported in [Nazarov, 1987], by a high paleomagnetic stability of rocks. The magnetostratigraphic data on the Turonian–Campanian obtained from in situ studies of the Upper Cretaceous Tuarkyr section carried out in 1996 were summarized in [Guzhikov *et al.*, 1998]. The magneto-stratigraphic data on Coniacian–Campanian deposits of southern England [Montgomery *et al.*, 1998] are well consistent with the Tuarkyr data. Structurally, southern England and Tuarkyr belong to young epi-Hercynian platforms; however, as regards their facial characteristics, the Upper Cretaceous sections in these regions are somewhat different.

CHARACTERIZATION OF THE SECTION

The paleomagnetic investigations were carried out within the southwestern flank of the Tuarkyr anticline (Fig. 1), where all stages of the Upper Cretaceous, except for the Maestrichtian, are represented. The bedding is subhorizontal, with dip angles of no more than 2°. We examined natural exposures near the Kemal' well and Akkyr Range 150 and 160 km from the Turkmenbashi–Kizil-Kaya highway (Fig. 1a). Cenomanian deposits are exposed in a number of gullies on the southern side of the highway in the Kemal' well area. Turonian–Campanian deposits are fully exposed on the

northern side of the highway in the scarps of the Akkyr Range (Mount Kyr; Figs. 1a, 1b).

E.Yu. Baraboshkin comprehensively described the section and performed determinations of macrofauna; in particular, he substantiated the presence of the middle Cenomanian ammonitic zone of *Acanthoceras (Alternacanthoceras) jukesbrownei.* L.F. Kopaevich determined foraminiferal complexes of the Turonian–Campanian, which has made it possible to refine the zoning scheme of the Upper Cretaceous Tuarkyr deposits previously developed in [Kuznetsov and Titova, 1961; Tverskaya, 1963; Aliev *et al.*, 1970].

The upper Albian sandstones unconformably overlain by the Upper Cretaceous sequence (Fig. 2) outcrop near the Kemal' well. Here, phosphorite conglomerate with numerous redeposited relics of upper Albian ammonites and aucellas of the *Stoliczkaia dispar* zone is present at the Cenomanian base. The overlying part of the Cenomanian, represented by alternating loose and dense glauconite–quartz fine- to medium-grained bioturbated sandstones (members I–II), was observed in a series of gullies located 2–3 km westward. The top of member II represents a "solid bottom" surface with numerous semidissolved nuclei of large (up to 20–30 cm) *Acanthoceras (Alternacanthoceras) jukesbrownei*, which gives grounds for dating the deposits of this member at the middle Cenomanian zone of the same name, whereas the underlying member I is tentatively assigned to the middle Cenomanian due to the absence of obvious evidence of large gaps. Sandstones of member III and marls of member IV (arenaceous at the base) are tentatively assigned to the Turonian because Turonian deposits in this region immediately overlie sandstones containing *A. jukesbrownei* [Kuznetsov and Titova, 1961; Aliev *et al.*, 1970]. Deposits of the upper Cenomanian are apparently absent in the Tuarkyr section.

The overlying Turonian–Campanian deposits were studied at the foot and on slopes of the Akkyr Range (the Mount Kyr area). They are represented by alternating variegated marls, limestones, and calcareous clays, the marls being predominant (Fig. 2). The presence of solid-bottom (SB) surfaces, the predominant type and color of rocks, and the presence of macrofaunal relics (inocerams, urchins, and nautiloids) are used as the main criteria for dividing the Turonian–Campanian sequence into members. The age of the members was established from complexes of plankton and benthic foraminifera. Member V (the upper Turonian) is composed of rhythmically alternating light gray marls and pinkish limestones separated by SB surfaces. Members VI and VII (the upper Turonian–the base(?) of the lower

Coniacian) are represented by rhythmically alternating greenish gray marls and white and pinkish limestones. A mature, phosphatized and ocherous, SB surface that serves as a marker horizon is present at the top of member VI. Members VIII and IX (the upper Coniacian) are composed of alternating brown, green, and red marls and brick-red limestones. The variegated members X–XII (the lower Santonian) are represented by interbedded green, brown, red, pink, white, and mottled marls and dense pink, white, and grayish white limestones. Members XIII (dense red and pink limestones with clay interbeds), XIV (alternation of red and mottled marls with pink (up to red) limestones), and XV (alternation of white, greenish, and pink marls with white and pink limestones) correlate with the upper Santonian. The upper part of member XV; member XVI, of dense white and light gray limestones that form a characteristic bench on the Akkyr Range slopes; and member XVII, represented by interbedded white limestones and gray-green marls are assigned to the lower Campanian. Members XVIII–XXII (alternating pink marls; pinkish, light gray and white limestones; and greenish calcareous clays) belong to the upper Campanian. They are overlain by Pliocene marls. The total thickness of the section is about 170 m.

The problems of zonal differentiation of the Turonian–Campanian deposits in this region and a comprehensive geological description of the section are the subject of a special paper.

EXPERIMENTAL POCEDURE

Paleomagnetic samples were taken from 32 stratigraphic levels in the Kemal' well area and from 118 stratigraphic levels of an outcrop in the Akkyr Range (Mount Kyr). The sampling interval varied from 0.5 to 1 m for the Kemal' section and from 1 to 1.2 m for the Akkyr section (Fig. 2). This sampling was complemented by the geological description of the section and the collection of paleontological samples. One paleomagnetic hand sample was taken from each level. Each hand sample was sawn into three or four 20-mm cubes. The magnetic susceptibility (K) was measured in detail on the Akkyr Range outcrop (the Turonian–Campanian) at a step of 20 cm (five K measurements per level).

In laboratory conditions, the paleomagnetic samples were studied with the standard complex of procedures [Khramov, 1982; Molostovskii and Khramov, 1997]: K and the natural remanent magnetization (NRM, or J_n) measurements, temporal and thermal demagnetizations, measurements of normal magnetization curves

Fig. 2. Magnetostratigraphic Tuarkyr section of the Cenomanian–Santonian. The members are enumerated in accordance with the description of E.Yu. Baraboshkin: (*1*) normal polarity; (*2*) reversed polarity; (*3*) "transitional" zones corresponding to anomalous directions; (*4*) absence of data on polarity; (*5*) "solid bottom" surfaces; (*6*) washout surfaces; (*7*) phosphorites; (*8*) shelly detritus; (*9*) bioturbations; (*10*) inclined bedding; (*11*) loose sandstone; (*12*) dense sandstone; (*13*) carbonate clay; (*14*) marl; (*15*) sandy marl; (*16*) limestone; (*17*) findings of ammonites; (*18*) microfauna samples.
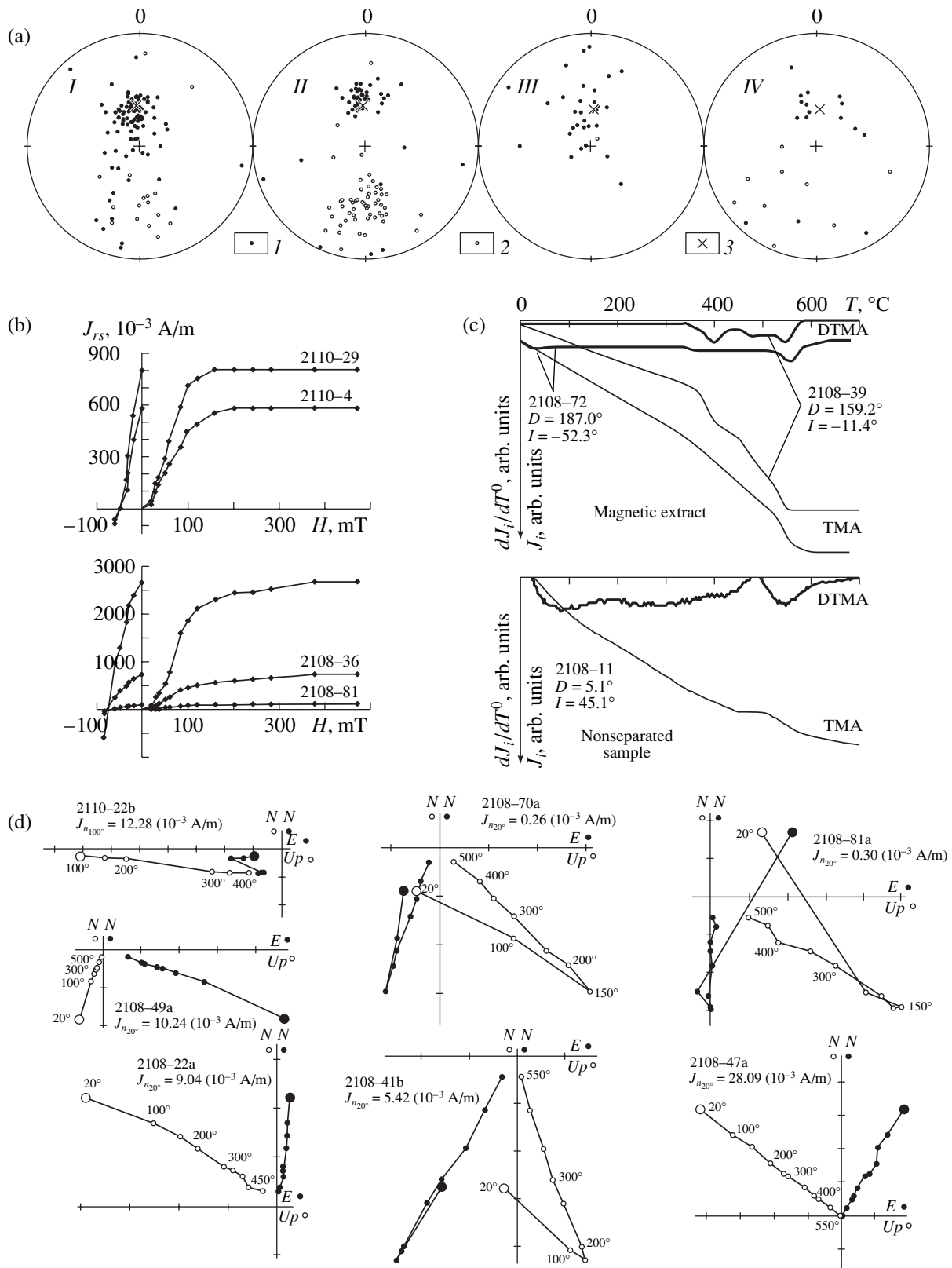
Fig. 3. Results of magnetic–mineralogical and component analyses. (a) Stratigraphic image of NRM vectors after temporal (*I, III*) and thermal (*II, IV*) demagnetizations of samples from the exposure of the Akkyr Range (*I, II*) and Kemal' well (*III, IV*): (*1*)–(*4*) vector projections in the (*1*) horizontal and (*2*) vertical planes and onto the (*3*) lower and (*4*) upper hemispheres; (*5*) direction of the present geomagnetic field ("remagnetization cross"). (b) Magnetic saturation curves. (c) TMA and DTMA curves. (d) Zijderveld diagrams.

and the remanent saturation magnetization (J_{rs}), determination of the saturation fields (H_s) and coercivity (H_{cr}), and thermomagnetic and differential thermomagnetic analyses (TMA and DTMA).

The remanent magnetization was measured with a JR-4 spinning magnetometer; the magnetic susceptibility was measured with IMV-2 (in the laboratory) and KT-5 (in situ) instruments. The TMA curves were constructed from the inductive magnetization (J_i), measured with a "magnetic balance" at the RIG SSU laboratory (using magnetic extracts in a field of 70 mT) and at Borok Geophysical Observatory, Schmidt United Institute of Physics of the Earth, Russian Academy of Sciences (using nonseparated samples in a field of 400 mT).

The temporal demagnetization consisted in keeping all samples within three-layer Permalloy containers for one month. The thermal demagnetization was performed in a kiln designed by V.P. Aparin. All samples were heated successively to temperatures changing from 100 to 350–550°C at a step of 50°C over 1–2 h. To account for a possible magnetic bias, two cubes from each hand sample having opposite orientations in two components of the vector J_n were placed into the kiln. If the remanent magnetization became comparable with the threshold sensitivity of the instrument, further heatings were not applied. Results of the paleomagnetic measurements were rejected from the subsequent analysis, if heatings failed to remove, at least partially, the secondary J_n component coinciding in direction with the present geomagnetic field or if laboratory magnetic bias was observed. (In the latter case, the paleomagnetic vector trajectories in stereographic projections measured in duplicate cubes differed substantially and the NRM value generally increased by a few times.) Determinations from 7 Kemal' hand samples and 11 Akkyr hand samples were rejected for these reasons.

The component analysis was performed by using Zijderveld diagrams and stereographic images of the J_n trajectories obtained during demagnetization procedures. Paleomagnetic directions, whose projections after the series of demagnetizations formed two isolated sets, in northern bearings on the lower hemisphere and in southern bearings on the upper hemisphere (Fig. 3a), were interpreted in terms of N and R polarities, respectively. Vectors with anomalous directions were interpreted as belonging to transition zones if they lay near the boundaries of magnetic zones of opposite polarities or to excursions if they were within a single-polarity zone, provided that all NRM components except for the stable one were completely removed, which was established from the Zijderveld diagrams. The anomalous directions were ignored in the statistical calculations, accomplished separately for the N and R samplings. For the resulting sampling, we took one paleomagnetic vector from each stratigraphic level, obtained by averaging over duplicate cubes if their final demagnetization results were similar. Otherwise, we took the result from a cube with better quality of the Zijderveld diagrams.

The samplings of the resulting NRM vectors were tested for their correspondence to the Fisher distribution by using the procedure proposed by Bazhenov and Ryabushkin [1978]. The conformity to the Fisher distribution is evidence for a one-component magnetization with random deviations of its directions from the average. The procedures of calculating the concentration and the confidence oval around the average, testing the hypotheses on coincidence of average directions or concentrations, etc., are correct only if the initial set is consistent with the Fisher distribution [Bazhenov and Ryabushkin, 1978; Khramov, 1982].

The standard in situ folding and pebble tests for substantiating the ancient nature (primary origin) of the identified magnetization components were inapplicable due to lacking a priori information. Therefore, we focused on the analysis of paleomagnetic characteristics as a function of lithological, mineralogical, and petromagnetic evidence and on the traditional magnetostratigraphic criterion of the external convergence.

EXPERIMENTAL RESULTS

The study rocks possess a weak magnetic susceptibility ($4-24 \times 10^{-5}$ SI units). The J_n values measured after the temporal demagnetization vary within a wider range: from 0.04×10^{-3} to 22.8×10^{-3} A/m. The Koenigsberger parameter (Q factor) calculated from these values varies from 0.01 to 2.85 (Fig. 2).

The thermomagnetic analysis was applied to ten samples with different polarities of J_n, representing various lithologies. The TMA and DTMA results point to the presence of Fe_3O_4, determined from the magnetization decay near 550°C (Fig. 3c). Natural magnetites usually do not have the Curie point (T_C) of pure Fe_3O_4 (578 K). Typically, their T_C values are appreciably lower due to various isomorphic admixtures in the magnetite crystal structure. The fine structure of the mineral and its weathering are responsible for a magnetization decrease within a wide range of temperatures. Weathered magnetite is often accompanied by maghemite, and the presence of this secondary ferromagnetic mineral is responsible for a noticeable drop of magnetization in the region of 400–500°C [Burov and Yasonov, 1979]. Therefore, the peak observed near 400°C (Fig. 3c) in the DTMA curve obtained from the magnetic extract of sample 2108-39 can be related to maghemite.

Samples from 115 stratigraphic levels were subjected to magnetic saturation. The artificial magnetization data (Fig. 3b) indicate the ubiquitous presence in the rocks of a phase generally characterized by the values $H_s = 200-400$ mT and $H_{cr} = 40-150$ mT. Such values of saturation parameters are typical of finely dispersed or partially oxidized magnetite [Tretyak, 1983], although they can be met in other minerals as well.

Table 1

	Lithological members and their ages														
	I–III s-$t_{(?)2}$		IV–VI $t_{(?)2}$–cn_1		VII–IX cn	X–XII st_1		XIII–XV st_2–km_1		XVI–XVII km_1	XVIII–XXII km_2		IV–IX t–cn	X–XXII st–km	
	N	R	N	R	N	N	R	N	R	R	N	R	N	R	N
D, deg	356.3	193.2	11.7	185.8	2.3	4.0	197.1	7.6	194.4	187.0	15.2	192.4	0.6	187.9	9.9
I, deg	57.0	−29.1	56.4	−39.4	48.6	49.9	−26.6	49.1	−45.8	−43.2	53.5	−34.8	48.2	−46.5	49.8
k	13.1	3.4	24.3	7.0	60.4	95.0	19.2	44.2	13.9	17.8	34.1	13.5	44.0	40.0	47.4
a_{95}, deg	10.7	21.9	10.7	30.5	4.7	7.2	8.9	8.0	8.4	8.2	7.6	15.5	8.0	4.3	5.9
n	13	12	7	3	15	4	13	7	20	16	10	6	7	26	12
S, deg	149.7		162.6			154.6		174.3			161.2			176.4	
$V_{n(D)}$	1.23	2.08	1.48		0.81		0.88	0.92	1.07	1.03	1.12		0.82	0.84	0.96
$V_{n(I)}$	0.56	0.30	0.39		0.55		0.01	0.78	0.01	0.01	0.65		0.77	0.04	0.87
														H_{cr} = 40.4–141.0 mT	

Note: N and R, normal and reversed polarities; ($D°$, $I°$), average paleomagnetic direction; k, interbed precision parameter; $a_{95}^{°}$, 95% confidence interval; n, number of samples; S, distance between the N and R vector averages; $V_{n(D)}$ and $V_{n(I)}$, respective criteria for estimating the correspondence of the azimuthal and radial distributions to the Fisher distribution [Bazhenov and Ryabushkin, 1976]; H_{cr}, coercive force; s, Cenomanian; t, Turonian; cn, Coniacian; st, Santonian; km, Campanian.

However, the fact that the stable component of magnetization persists to 550°C invalidates the assumption that iron hydroxide, maghemite, and other ferromagnetic species are carriers of the stable component of magnetization. The presence of hematite was not fixed in any of the DTMA curves. Therefore, the joint results of the normal magnetization experiments and thermomagnetic analysis indicate that magnetite should be recognized as the most probable carrier of the stable component of magnetization.

Paleomagnetically, the Upper Cretaceous Tuarkyr section is distinctly subdivided into two nonequivalent parts coinciding with its lithological differentiation; these are intervals of low-stability magnetization (sandy members I–III, of Cenomanian (+ Turonian?) age) and of high-stability magnetization (carbonate–clayey members IV–XXII, of the Turonian–Campanian). In the majority of Zijderveld diagrams from samples of the Cenomanian sandstones, the lines fixing the high-temperature vector variations do not tend toward the center of coordinates (Fig. 3d, sample 2110-22b). Such a situation can be due to an incomplete removal of the secondary (low-temperature) component of J_n, which is the reason why the resulting samplings of vectors are characterized by low interbed concentrations and poor agreement with the hypothesis on the Fisher distribution, whereas the difference between the averages of paleomagnetic R and N polarity directions differs significantly from 180° (Table 1). The carbonate–clayey Turonian–Campanian deposits (observation point 2108) are characterized by a better quality of the paleomagnetic signal. They generally record a two-component NRM: its first component is completely removed at temperatures of 150–200°C and, judging from its closeness to the direction of remagnetization by the present field, is associated with products of oxidation of magnetite grains; the second, stable component persists up to 550°C and is likely to be of ancient origin (Fig. 3d). The Turonian–Campanian interbed precision parameters are 3–5 times higher than the Cenomanian values, and the average Turonian–Campanian paleomagnetic directions of the N and R polarities are nearly antiparallel (Table 1).

Taking into account large distinctions in the degree of paleomagnetic reliability, different approaches were applied to constrain the origin of the resulting J_n vectors from the sandy (Cenomanian) and carbonate–clayey (Turonian–Campanian) parts of the section. Only the polarity sign independence of lithological, mineralogical, and petromagnetic characteristics was checked in the Cenomanian interval, and the criterion of the external convergence was applied. In addition to this, the precision parameters (k), paleomagnetic inclinations (I), and distances between the paleomagnetic vector and the direction of remagnetization by the present field (Δ) were examined as a function of petromagnetic characteristics (k, J_{rs}, and H_{cr}) in the Turonian–Campanian interval.

The paleomagnetic statistics was calculated separately for sets of members characterized by similar lithologies and ages (Table 1). Seven anomalous directions were excluded from the sets analyzed (six of them are confined to the boundaries of magnetic zones, and one lies inside the R zone; Fig. 2). Explicit dependences of paleomagnetic characteristics on the age of deposits and their lithology are not observed within members IV–XXII (the Turonian–Campanian).

The Turonian–Campanian rocks (members IV–XXII) cannot be correctly divided into separate lithological groups (carbonate clays, marls, and limestones) without an expensive chemical analysis. This circumstance makes it impossible to analyze the dependence of paleomagnetic precision parameters and inclinations on the concentrations of terrigenous (carbonate) material in the rocks. However, the comparison of paleomagnetic precision parameters with the coercive force values revealed evident regular patterns (Fig. 4a): the maximum precision parameters[2] for the R directions (38.0–44.9) correlate with minimum values of H_{cr}, whereas k minimums (10.0–13.4) correlate with H_{cr} maximums. The coefficients of linear correlation between the precision parameters and the H_{cr} values (for both R and N polarities) are significant at a level of 0.01 (Table 2). It is noteworthy that the precision parameter values for vectors of opposite polarities virtually coincide in the region of small H_{cr} values (Fig. 4a). The stereographic image of the vectors corresponding to this region (outlined in Fig. 4a) is presented in Fig. 4b.

The coercivity H_{cr} increases with increasing intensity of oxidation (martitization) of magnetic grains and/or with decrease in their size. Under conditions of the arid climate of Turkmenistan, all particles of Fe_3O_4 in natural exposures are, to an extent, oxidized, so that a secondary chemical component (J_{rc}) is present in each sample. A regular decrease in the concentrations of R vectors associated with high H_{cr} values is due to a more substantial contribution of J_{rc} to the total NRM as compared with small values of H_{cr}. On the contrary, the concentration of paleomagnetic directions in normally magnetized samples increases at high H_{cr} values due to the prevalence of J_{rc}, because the directions of J_{rc} coinciding with the present field and of the stable N-polarity component J_n are similar, which prevents their separation by component analysis. If this model is valid, a direct correlation must take place between the parameters H_{cr} and I, and an inverse correlation, between H_{cr} and Δ, for both polarities, and this is precisely what is

[2] The procedure of calculating the paleomagnetic precision parameter was performed in the following way: all paleomagnetic directions were grouped in ascending order of their corresponding H_{cr} values. The precision parameters were calculated with a moving window of 15 samples in size at a one-sample step. Since the number of samples subjected to the experiments of normal saturation was limited, not all paleomagnetic directions were involved in this analysis.
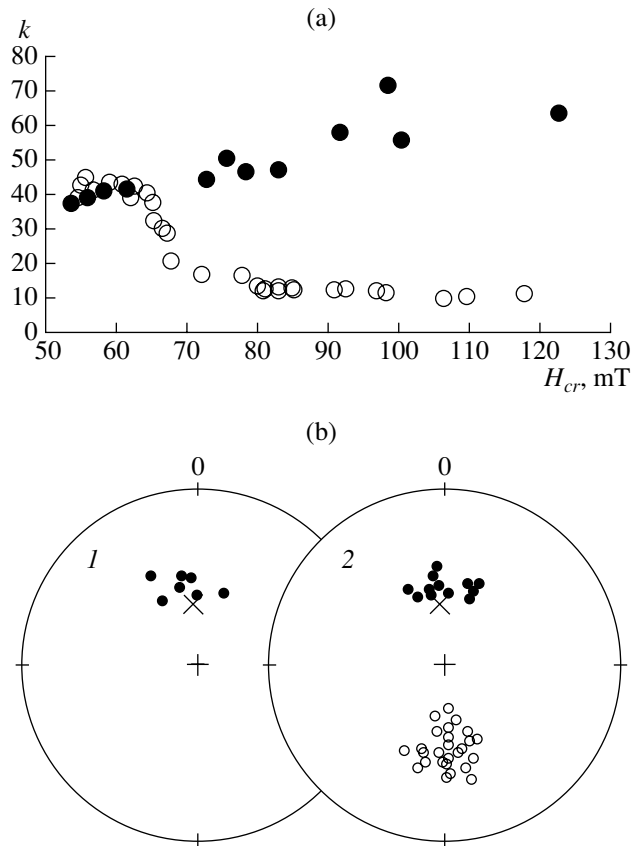
Fig. 4. (a) The H_{cr} dependence of concentrations of paleomagnetic vectors (open and solid circles refer to the R and N polarities, respectively). Outlined is the region where the concentrations of R and N vectors are similar (38.0–44.9). (b) Stereograms of the NRM vectors corresponding to the range of low H_{cr} values for the (*1*) Turonian–Coniacian and (*2*) Santonian–Campanian.

observed in reality (Table 2). Evidently, the "purest" paleomagnetic vectors of either polarity concentrate in the region of low H_{cr} values, where the corresponding paleomagnetic concentrations are nearly the same (from 38.0 to 44.9; Fig. 4a). The paleomagnetic statistics calculated for these vectors is presented in the last three right-hand columns of Table 1. The J_n averages for groups of opposite polarities in the Santonian–Campanian interval (members X–XXII) are virtually antiparallel because the averages of the N sampling and of R vectors rotated through 180° are statistically indistinguishable. The test of Shipunov [1993] for the coincidence of average directions of the two sets is positive at a significance level (*p*) of 0.01 (the statistic $F_2 = 0.12$ is smaller than the criterion $(1/p)^{1/(N-2)} - 1 = 0.14$). Preliminarily, we checked whether the precision parameters of these sets coincide at $p = 0.01$ (the statistic is $k_1/k_2 = 1.18$) [Shipunov, 1993].

Analysis of the dependences of K, I, and Δ on K and J_{rs} shows that, in the case of R directions, a significant negative correlation is observed for the pairs K–Δ, J_{rs}–Δ,

Table 2

Paleomag-netic parameters	R polarity		N polarity	
	n	coefficient of linear correlation	n	coefficient of linear correlation
$H_{cr}-k$	32	−0.87	13	0.89
$H_{cr}-I$	46	0.31	27	0.40
$H_{cr}-\Delta$	46	−0.40	27	−0.34
$K-k$	44	−0.32	31	0.80
$J_{rs}-k$	32	−0.42	13	0.92
$K-I$	56	0.32	44	−0.24
$J_{rz}-I$	46	0.30	27	−0.13
$K-\Delta$	56	−0.34	44	−0.06
$J_{rs}-\Delta$	46	−0.30	27	−0.07

Note: k, interbed precision parameter; Δ, distance between the paleomagnetic vector and the direction of remagnetization by the present field; I, paleomagnetic inclination; K, magnetic susceptibility; J_{rs}, remanent saturation magnetization; H_{cr}, coercive force; n, number of samples.

$K-k$, and $J_{rs}-k$, whereas a significant positive correlation takes place for the pairs $K-I$ and $J_{rs}-I$ (Table 2). The value of the remanent saturation magnetization is mainly controlled by the concentration of the ferromagnetic fraction. Given magnetic susceptibilities of up to 20×10^{-5} SI units (which are actually observed in the study section), the contribution of paramagnetic species to the K value can be appreciable. However, if it were predominant, the relationships of paleomagnetic characteristics with K and J_{rs} would be dissimilar, which is not the case (Table 2). This can be regarded as evidence that variations in the magnetic susceptibility are mainly due to variations in the concentrations of ferromagnetic material contents. The fact that the highest precision parameters of the R direction are observed in the range of minimum values of K and J_{rs} implies that the "purest" stable NRM components are confined to weakly magnetic samples (mostly limestones, as is evident from visual examination). Probably, magnetite grains in dense limestones are least subjected to oxidation. Moreover, Bazhenov [1983] showed that the paleomagnetic inclination in limestones is virtually not underestimated, because they did not experience any noticeable compaction at the stage of diagenesis. It is reasonable to suggest that the martitization of magnetite grains was more intense in terrigenous, rather than carbonate, varieties. Although the oxidation of the ferromagnetic fraction decreases the K and J_{rs} values insignificantly, it results in the formation of a hard chemical component of magnetization. In this context, low concentrations of R directions observed in more magnetic marls and clays are natural. On the other hand, the concentrations of N vectors must rise with an increase in K and J_{rs} due to a stronger influence of J_{rc}. The actual data corrobo-

rate the presence of a strong positive correlation for the pairs $K-k$ and $J_{rs}-k$ in the set of N vectors (Table 2). However, the coefficients of linear correlation for the pairs $K-\Delta$, $J_{rs}-\Delta$, $K-k$, $J_{rs}-k$, $K-I$, and $J_{rs}-I$ are insignificant (even at a significance level of 0.10; see Table 2). The insensitivity of the correlation test in this case is probably connected with the small difference between the paleomagnetic direction and the vector of the present geomagnetic field, which is comparable to the determination uncertainty of the stable component of J_n.

Based on the results of our studies, we summarize the experimental evidence consistent with the hypothesis on the ancient age of J_n.

(1) The geomagnetic field reversal is a phenomenon of planetary scale. The probability of the coincidence of paleomagnetic boundaries with borderlines constrained by local and regional evidence is not very high in stratigraphically complete sections, provided that the magnetization is primary. Therefore, the fact that magnetic zones are independent of lithological and mineralogical features is more favorable for the hypothesis relating the sign of J_n to an ancient field regime than the coincidence of lithology and polarity changes. The absence of any correlation of the polarity sign with boundaries of lithological members and other features characterizing the material composition (the carbonate content, color of rocks, petromagnetic parameters, etc.) is evident in the section studied (Fig. 2).

(2) The substantiation of a detrital (postdetrital) nature of magnetization is equivalent to the substantiation of the primary origin of the latter. The following regular patterns, more characteristic of the detrital NRM rather than J_{rc}, are observed in the section studied:

(a) The values of the factor Q are typically small in the rocks (hundredths and tenths of fractions of unity). The Q values are, as a rule, close to or slightly higher than unity in rocks in which the authigenic genesis of minerals responsible for magnetization is reliably established [Tretyak, 1983; Molostovskii and Khramov, 1997; Grishanov, 1996]. In the section studied, the values $Q > 1$ are recorded only at 15 levels and can, with equal probability, characterize both N and R polarities. Even if the paleomagnetic determinations with $Q > 1$ are rejected, this will not change the general paleomagnetic structure of the section.

(b) The paleomagnetic interbed precision parameters are relatively small, amounting to a few tens (Table 1).

(c) The observed dependences of k, I, and Δ on H_{cr} (Fig. 4a; Table 2) can be interpreted in terms of the presence of either the primary component of J_n or a metachronous bipolar component of magnetization whose direction is distorted in samples with intensely

oxidized magnetite grains due to an incomplete removal of J_{rc}.

(d) The most satisfactory paleomagnetic results are related to weakly magnetic limestones, which is in good agreement with the model of postdetrital (diagenetic) formation of the magnetization.

(3) The difference between the average directions of the paleomagnetic normal- and reversed-polarity vectors is close to 180° in both the entire section (except for members I–III, where the removal of stable components is obviously incomplete) and individual intervals. The average directions are virtually antiparallel for the sets of the "purest" components. The presence of directions of two polarities in the section, a 180° difference (within the determination uncertainty) between these directions, and the coinciding precision parameters of the N and R sets are traditionally regarded as weighty arguments in favor of both the quality of paleomagnetic determinations and the primary nature of magnetization (reversal test) [Molostovskii and Khramov, 1997; Van der Voo, 1993].

Each of the above features, when taken alone, does not prove the primary origin of magnetization; however, considered together, they are more consistent with the hypothesis of primary magnetization than with any other assumption, for example, the hypothesis of a bipolar metachronous NRM.

The criterion of external convergence, i.e., the coincidence of paleomagnetic structures in coeval deposits of various (preferably widely separated) sections is very important evidence of an ancient nature of magnetization. Larger differences between the compared sections in their lithological, facial, and structural characteristics increase the value of the external convergence factor as a proof of the primary nature of J_n. On the whole, the paleomagnetic structure of the Tuarkyr section is in good agreement with the data on the Upper Cretaceous in other regions (Fig. 5), which is discussed in the next section.

DISCUSSION OF RESULTS

The paleomagnetic column is subdivided into a reversed polarity subzone Rs_2 associated with the middle(?) Cenomanian (members I–II) and three orthozones: lower, with a predominantly normal polarity ($NrK_2t–cn$); middle, with a prevailing reversed polarity ($RnK_2st–km_1$); and upper, with a variable polarity (NRK_2km_2). These orthozones correspond to the upper(?) Turonian–Coniacian (members III–IX), Santonian–lower Campanian (members X–XVII), and upper Campanian (members XVIII–XXII). The magnetostratigraphic comparison of the Upper Cretaceous of various regions (Fig. 5) presented below makes it possible to identify several magnetic zones discovered in the Tuarkyr section with the known paleomagnetic units and to refine the stratification of the section and the amount of sedimentation breaks.

The subzone Rs_2 is evidently an analogue of the middle Cenomanian R subzone, previously established within the *A. rhotomagense* zone in the North Caucasus (Fig. 5-V) and Kopet Dagh (Fig. 5-VI). The normal polarity of members III and IV is likely evidence of their upper Turonian age, because the lower Turonian is characterized by a large R subzone (Fig. 5-V). The two closely spaced thin zones of opposite polarities within member IV possibly correspond to the upper Turonian r microzone and/or the lower Coniacian R subzone that were revealed in Dagestan (Fig. 5-VI). The last variant of correlation seems preferable, because R intervals are also recorded in the lower Coniacian of southern England (Fig. 5-IV). From this standpoint, Tuarkyr members VI–VII must be assigned to the lower Coniacian. Analogues of the upper Coniacian (Klyuevskaya) R subzone are unambiguously absent in the study section, as is evident from the washout of the *I. labiatus* and partially the *I. mantelly* inoceram zones. The $RnK_2st–km_1$ orthozone undoubtedly correlates with anomaly 33 (the Kul'dzhinskaya R orthozone; Figs. 5-I, II), because no evidence on other large R intervals in the Santonian–Campanian is available. As is generally acknowledged at present, the reversed polarity is characteristic of both the lower Campanian and the upper Santonian. This fact is corroborated by data from Canada (Fig. 5-VII) and European Russia (Fig. 5-VIII) and is reflected in the recent versions of magnetochronological scales (Fig. 5-II). The data on the predominance of R polarity in the lower Santonian contradict the well-known magnetostratigraphic evidence from North Mediterranean sections (Fig. 5-IX–XI) but basically agree with the polarity zonation of the lower Santonian of England, the Caucasus, and Kopet Dagh (Fig. 5-IV–VI). The correlation of the NRK_2km_2 orthozone presents no difficulties. The upper Campanian is everywhere characterized by an intricate paleomagnetic zonation. Comparison of the upper Campanian sections of Tuarkyr and southern England (Fig. 5-III, IV) reveals an obvious similarity between their paleomagnetic columns. Chrons $C32$ and partially $C31$ (Fig. 5-II) are probable analogues of NRK_2km_2 in the magnetochronological scale.

Therefore, the magnetostratigraphic evidence for the Turonian–Campanian of Tuarkyr is in good agreement with data on deposits of the same age in the Kopet Dagh, the North Caucasus, and southern England. The presence of reversals in the Cenomanian, Turonian, and Coniacian is also supported by data from the Chukot Peninsula, Germany, the southern Alps, and North Africa (Fig. 5-XII–XV).

Substantial divergences between the ideas of the paleomagnetic structure of the Cenomanian–Campanian section interval arise when the Tuarkyr section is compared with North Mediterranean sections; the calibration of the latter with the use of the sequence of linear anomalies underlies the present magnetochronological scales. The normal polarity alone characterizes the
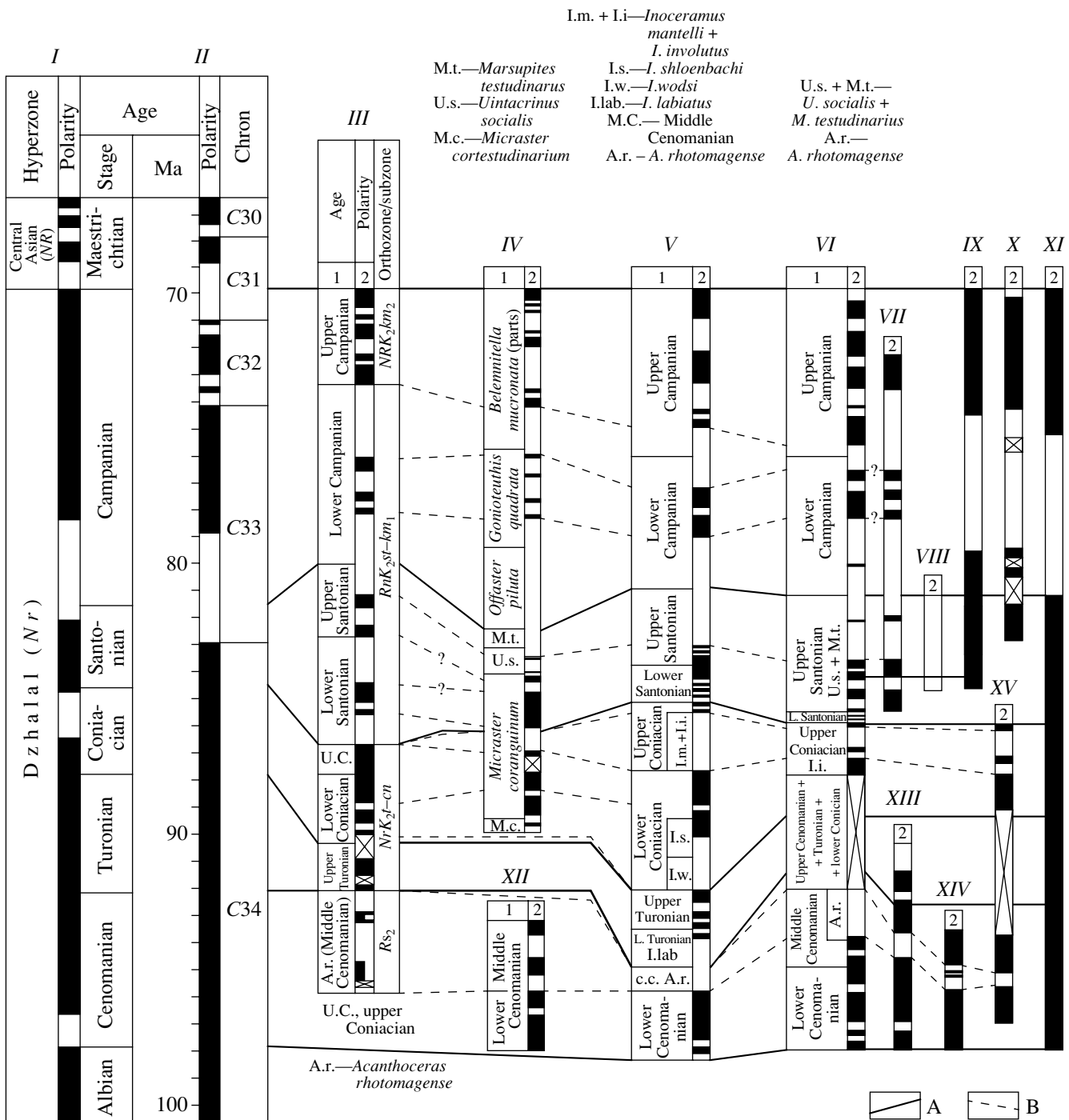
Fig. 5. Comparison of magnetostratigraphic data for the Cenomanian–Campanian: (*I*) magnetostratigraphic time scale [Molostovskii and Khramov, 1984]; (*II*) magnetochronological scale [Gradstein and Ogg, 1996]; (*III*) Tuarkyr (this work); (*IV*) southern England [Montgomery *et al.*, 1998]; (*V*) Northern Caucasus, composite Aimaki section of village of Aimaki (Dagestan) and Bass River (Chechnya) [Fomin and Eremin, 1993, 1999; Fomin, 2000]; (*VI*) Western Kopet Dagh, the composite section of Kanavchai gorge (Kazandzhik), village of Kara-kala, and Kamyshly spring (Kyzyl-Arvat) [Eremin *et al.*, 1995; Fomin and Eremin, 1999; Fomin and Molostovskii, 2001]; (*VII*) southwestern Alberta (Canada) [Leahy and Lerbekmo, 1995]; (*VIII*) Lower Volga region, Nizhnyaya Bannovka section [Pechersky *et al.*, 1983]; (*IX*) Southern Alps (Italy) [Channel and Medizza, 1981]; (*X*) Apennines [Lambert *et al.*, 1997]; (*XI*) Southern Alps (Italy) and Apennines, composite section [Lowrie *et al.*, 1980]; (*XII*) Ruhr region (Germany), composite section [Hambach and Krumsiek, 1989]; (*XIII*) Southwestern Morocco, composite section [Krumsiek, 1982]; (*XIV*) Southern Alps (Italy) [Vandenberg and Wonders, 1980]; (*XV*) Chukot Peninsula, Ugol'naya Bay section [Pergament *et al.*, 1971]; (*A*) correlation lines of stage boundaries; (*B*) paleomagnetic correlation lines. For polarity notation, see Fig. 2.

Cenomanian–Santonian of these scales (Fig. 5-IX–XI). However, the "standard" sections are located in the zone of intense tectonic deformations and have features indicating metamorphization of rocks, which increases the probability of their regional overprinting. Moreover, the foraminiferal and nannoplanktonic scales are mainly used for their differentiation, whereas these scales are not always unambiguously correlated with the ammonitic and belemnitic scales. Lack of space prevents us from discussing the reasons why linear anomalies can fail to records some of the Cenomanian–Santonian reversals; however, this is analyzed in sufficient detail in [Gorodnitskii, 1996, 1998; Gordin, 2000].

CONCLUSION

The main result of our work is the inference that the paleomagnetic structure of the Cenomanian–Campanian interval of the time scale is more complicated as compared with the traditional ideas. The existence of the middle Cenomanian R subzone, the presence of reversals in the Coniacian, and the prevalence of reversed polarity in the Santonian–Campanian have been confirmed. In this connection, the concepts of a predominant single-polarity regime of the Cenomanian–Campanian field and the structure of the Cretaceous paleomagnetic time scale need revision. The upper boundary of the Dzhalal hyperzone and the top of the $C34$ chron should be lowered to approximately the base of the Santonian. The evidence presented in this paper, of course, needs further verification and refinement. If it is corroborated, the problem of revising the geodynamic models accounting for the coincidence of the "Cretaceous superchron of normal polarity" with various global geological events will naturally arise [Didenko, 1998; Milanovskii, 1996; Larson and Olson, 1991; and others]

ACKNOWLEDGMENTS

REFERENCES

Aliev, M.M., Pavlova, M.M., and Zabelina, T.M., Stratigraphy of the Upper Cretaceous in Western Turkmenistan, *Yurskie, melovye i paleogenovye otlozheniya zapada Srednei Azii* (The Jurassic, Cretaceous, and Paleogene of Western Central Asia), M.M. Aliev, Ed., Moscow: Nauka, 1970, pp. 64–105.

Bazhenov, M.L., Paleomagnetic Direction Implications of Lithology in Cretaceous and Paleocene Deposits of the Western Kopet Dagh, *Izv. Akad. Nauk SSSR, Fiz. Zemli*, 1983, no. 8, pp. 67–75.

Bazhenov, M.L. and Ryabushkin, P.K., Application of Statistical Convergence Tests in Paleomagnetic Studies, *Izv. Akad. Nauk SSSR, Fiz. Zemli*, 1978, no. 7, pp. 100–104.

Burov, B.V. and Yasonov, P.G., *Vvedenie v differentsial'nyi termomagnitnyi analiz gornykh porod* (Introduction to the Differential Thermomagnetic Analysis of Rocks), Kazan: Kazan Univ., 1979.

Channel, J.E.T. and Medizza, F., Upper Cretaceous and Palaeogene Magnetic Stratigraphy and Biostratigraphy from the Venetian (Southern) Alps, *Earth Planet. Sci. Lett.*, 1981, vol. 55, pp. 419–432.

Didenko, A.N., The 100-m.y. Variations in the Paleozoic and Implications for Core–Lithosphere Coupling, *Izvestiya, Phys. Solid Earth*, 1998, vol. 34, pp. 351–358.

Eremin, V.N., Nazarov, Kh., Ramazanov, S.A., and Fomin, V.A., Magnetostratigraphy of the Upper Cretaceous Kanavchai Key Section (Western Kopet Dagh), *Izv. Akad. Nauk Turkm.*, 1995, no. 4, pp. 163–169.

Fomin, V.A., Upper Cretaceous Magnetostratigraphy of the Dzhalal Hyperzone, *Paleomagnetizm i magnetizm gornykh porod: teoriya, praktika, eksperiment. Tez. dokl. Borok, 25–29 sent. 2000 g.* (Paleomagnetism and Magnetism of Rocks: Theory, Practice, and Experiment. Abstracts Conf. Borok, Sept. 25–29, 2000), V.P. Shcherbakov, Ed., Moscow: GEOS, 2000, pp. 63–64.

Fomin, V.A. and Eremin, V.N., Magnetostratigraphy of the Upper Cretaceous in the Southern USSR, *Voprosy stratigrafii paleozoya, mezozoya i kainozoya* (Stratigraphy of the Paleozoic, Mesozoic, and Cenozoic), G.V. Kuleva and V.G. Ochev, Eds., Saratov: Saratov Univ., 1993, pp. 134–142.

Fomin, V.A. and Eremin, V.N., Magnetostratigraphic Correlation of the Santonian–Campanian Magnetic R-Zone in Sections of the North Caucasus and Western Kopet Dagh *Sbornik nauchn. tr. NII geologii SGU. Nov. ser.* (Collection of Scientific Papers of the Research Institute of Geology, Saratov State University. New Series), Yu.P. Kontsenebin *et al.*, Eds., Saratov: GosUNTs "Kolledzh," 1999, vol. 1, pp. 79–84.

Fomin, V.A. and Molostovskii, E.A., Magnetostratigraphy of the Cenomanian in Western Turkmenistan, *Byull. Mosk. O-va Ispyt. Prir. Otd. Geol.*, 2001, vol. 76, no. 4, pp. 62–70.

Gordin, V.M., Interpretation of the Anomalous Magnetic Field of Oceans after Vine and Mathews, *Tektonika, geodinamika i protsessy magmatizma i metamorfizma. Materialy soveshchaniya. T. 1* (Tectonics, Geodynamics, and Processes of Magmatism and Metamorphism. Conf. Proc.), Moscow: GEOS, 2000, vol. 1, pp. 168–170.

Gorodnitskii, A.M., Ed., *Priroda magnitnykh anomalii i stroenie okeanicheskoi kory* (The Origin of Magnetic Anomalies and the Structure of the Oceanic Crust), Moscow: VNIIRO, 1996.

Gorodnitskii, A.M., The Origin of Magnetic Anomalies and the Oceanic Crust Structure at Slow-Rate Spreading Ridges, *Izv. Sektsii Nauk o Zemle RAEN*, 1998, no. 1, pp. 152–176.

Gradstein, F. and Ogg, J., A Phanerozoic Time Scale, *Episodes*, 1996, vol. 19, nos. 1/2.

Grishanov, A.N., Authigenic Magnetic Mineralization in Deposits of Oil-Bearing Structures of the Samara Volga Region, *Paleomagnetizm i magnetizm gornykh porod. Tez. dokl. Borok, 3–9 iyunya 1996 g.* (Paleomagnetism and Magnetism of Rocks. Abstracts Conf. Borok, June 3–9, 1996), A.N. Didenko, Ed., Moscow: OIFZ RAN, 1996, pp. 30–31.

Guzhikov, A.Yu., Molostovskii, E.A., Nazarov, Kh., *et al.*, Magnetostratigraphy of the Upper Cretaceous of the Akkyr Range (Tuarkyr, Turkmenistan), *Paleomagnetizm i magnetizm gornykh porod: teoriya, praktika, eksperiment. Tez. dokl. Borok, 26–30 okt. 1998 g.* (Paleomagnetism and Magnetism of Rocks: Theory, Practice, and Experiment. Abstracts Conf. Borok, Oct. 26–30, 2000), V.P. Shcherbakov, Ed., Moscow: GEOS, 1998, pp. 26–28.

Hambach, U. and Krumsiek, K., Eine Magnetostratigraphische Gliederung des Oberen Alb und Unteren Cenoman aus Kernbohrungen des Ruhrgebietes, *Geol. Jahrb.*, 1989, vol. A113, pp. 401–425.

Khramov, A.N., Ed., *Paleomagnitologiya* (Paleomagnetology), Leningrad: Nedra, 1982.

Krumsiek, K., Cretaceous Magnetic Stratigraphy of Southwest Morocco, *Geology of Northwest African Continental Margin*, Berlin, 1982, pp. 475–497.

Kuznetsov, V.I. and Titova, M.V., Stratigraphy of the Tuarkyr Upper Cretaceous, *Problema neftegazonosnosti Srednei Azii. Vyp. 2. Geologiya i neftegazonosnost' zapadnoi chasti Srednei Azii. Tr. VSEGEI, nov. ser.* (Oil and Gas Content in Central Asia. Issue 2. Geology and Oil and Gas Content in Western Central Asia. VSEGEI Proc., New Series), N.P. Luppov, Ed., Leningrad: Gostoptekhizdat, 1961, pp. 219–228.

Lampert, S.A., Lowrie, W., Hirt, A.M., *et al.*, Magnetic and Sequence Stratigraphy of Redeposited Upper Cretaceous Limestones in the Montagna della Maiella, Abruzzi, Italy, *Earth Planet. Sci. Lett.*, 1997, vol. 150, pp. 79–93.

Larson, R.L. and Olson, P., Mantle Plumes Control Magnetic Reversal Frequency, *Earth Planet. Sci. Lett.*, 1991, vol. 107, pp. 437–447.

Leahy, G.D. and Lerbekmo, J.F., Macrofossil Magnetobiostratigraphy for the Upper Santonian–Lower Campanian Interval in the Western Interior of North America: Comparisons with European Stage Boundaries and Planctonic Foraminiferal Zonal Boundaries, *Can. J. Earth Sci.*, 1995, vol. 32, pp. 247–260.

Lowrie, W., Channel, J.E.T., and Alvarez, W., A Review of Magnetic Stratigraphy Investigations in Cretaceous Pelagic Carbonate Rocks, *J. Geophys. Res.*, 1980, vol. 85, pp. 3597–3605.

Milanovskii, E.E., Correlation between the Geomagnetic Reversal Acceleration Phases, Ocean Level Drops, and Stronger Compressive Crustal Deformation Stages in the Mesozoic and Cenozoic, *Geotektonika*, 1996, no. 1, pp. 3–11.

Molostovskii, E.A. and Khramov, A.N., Phanerozoic Paleomagnetic Time Scale in Relation to Magnetostratigraphic Problems, *27 MGK. Moskva, 4-14 avg. 1994 g. Stratigrafiya. Doklady. T. 1* (Proc. Conf. MGK Moscow, Aug. 4–14, 1994. Stratigraphy), Moscow: Nauka, 1984, vol. 1, pp. 16–23.

Molostovskii, E.A. and Khramov, A.N., *Magnitostratigrafiya i ee znachenie v geologii* (Magnetostratigraphy and Its Implications for Geology), Saratov: Saratov Univ., 1997.

Montgomery, P., Hailwood, E.A., Gale, A.S., and Burnett, J.A., The Magnetostratigraphy of Coniacian–Late Campanian Chalk Sequences in Southern England, *Earth Planet. Sci. Lett.*, 1998, vol. 156, pp. 209–224.

Nazarov, Kh. and Mamedov, M., *Paleomagnetizm mezozoya i kainozoya Turkmenii* (Paleomagnetism of the Mesozoic and Cenozoic in Turkmenistan), Ashkhabad: Ylym, 1989.

Pechersky, D.M., Naidin, D.P., and Molostovsky, E.A., The Santonian–Campanian Reversed Polarity Magnetozone and the Late Cretaceous Magnetostaratigraphical Time-Scale, *Cretaceous Res.*, 1983, vol. 4, pp. 251–257.

Pergament, M.A., Pechersky, D.M., and Khramov, A.N., On the Paleomagnetic Time Scale of the Mesozoic, *Izv. Akad. Nauk SSSR, Ser. Geol.*, 1971, no. 10, pp. 3–11.

Shipunov, S.V., *Osnovy paleomagnitnogo analiza: teoriya i praktika* (Fundamentals of Paleomagnetic Analysis: Theory and Practice), Moscow: Nauka, 1993.

Shreider, A.A., Magnetic Chronology of the Ocean Floor, *Izvestiya, Phys. Solid Earth*, 1998, vol. 34, pp. 932–945.

Stratigraficheskii kodeks (Stratigraphic Code), St. Petersburg: VSEGEI, 1992.

Tretyak, A.N., *Estestvennaya ostatochnaya namagnichennost' i problema paleomagnitnoi stratifikatsii osadochnykh tolshch* (Natural Remanent Magnetization and the Problem of Magnetic Stratification of Sedimentary Sequences), Kiev: Naukova Dumka, 1983.

Tverskaya, L.A., Stratigraphic Distribution of Fossil Foraminifera Complexes in the Upper Cretaceous Tuarkyr Section, *Problema neftegazonosnosti Srednei Azii. Novye dannye po geologii zapadnoi chasti Srednei Azii. Tr. VSEGEI, nov. ser.* (Oil and Gas Content in Central Asia. New Data on the Geology of Western Central Asia. VSEGEI Proc. New Series), N.P. Luppov, Ed., Leningrad: Gostoptekhizdat, 1963, vol. 14, pp. 172–177.

Van der Voo, R., *Palaeomagnetism of the Atlantic, Tethys and Iapetus Oceans*, Cambridge: University Press, 1993.